THE ASTROPHYSICAL JOURNAL, 276:544–550, 1984 January 15

RADIO STRUCTURE OF THE PROTO-PLANETARY NEBULA GL 618

SUN KWOK
Herzberg Institute of Astrophysics, Ottawa; and Department of Physics, University of Calgary, Calgary

AND

R. C. BIGNELL
National Radio Astronomy Observatory, Socorro, New Mexico[1]
Received 1983 April 8; accepted 1983 June 20

ABSTRACT

Radio maps of the proto-planetary nebula GL 618 have been obtained with angular resolutions as high as 0.″07. A bright radio core of size 0.″4 × 0.″1 is found to be surrounded by a halo of several arc seconds in size. The core shows an elongated structure having the same symmetry axis as the optical reflection nebulosities. It is suggested that the ionized region of GL 618 is ionization bounded in the equatorial directions, and the bipolar morphology is the result of an anisotropic density distribution in the circumstellar envelope of its red-giant progenitor. The small angular size and high emission measure ($>10^{10}$ cm^{-6} pc) of the core suggest that GL 618 is a planetary nebula of extremely young age ($\sim 10^2$ yr).

Subject headings: nebulae: individual — nebulae: planetary — radio sources: general

I. INTRODUCTION

At the present time GL 618 is probably the best candidate for a proto-planetary nebula because it possesses the properties of both red-giant envelopes (RGE) and young planetary nebulae (PN). An expanding molecular envelope of $\sim 1'$ in size has been detected in CO (Lo and Bechis 1976) which resembles the molecular envelopes of red giants. The mass loss rate deduced from CO observations is very high ($\sim 2 \times 10^{-4}[D/1.5\ \mathrm{kpc}]^2\ M_\odot\ \mathrm{yr}^{-1}$, Knapp *et al.* 1982)[2] but comparable to the mass loss rates observed in high-mass ($M_{\mathrm{core}} \sim 1\ M_\odot$) stars at the very late stages of asymptotic giant-branch (AGB) evolution. The total luminosity of GL 618 ($\sim 1.8 \times 10^4[D/1.5\ \mathrm{kpc}]^2\ L_\odot$, Kleinmann *et al.* 1978) is also similar to luminosities of high-mass PNs. The central star of GL 618 has a temperature of $\sim$30,000 K (Westbrook *et al.* 1977; Calvet and Cohen 1978), again not unlike a young PN. A compact H II region ($\theta \sim 0.''3$) has been found, embedded in the central IR source (Wynn-Williams 1977; Kwok and Feldman 1981).

The two visible nebulosities separated by $\sim 7''$ along the east-west direction on each side of the IR source are probably reflection nebulae (Calvet and Cohen 1978). Carsenty and Solf (1982) estimate that these lobes are moving away from the central star at velocities of $\sim$80 km s^{-1} along directions which are $\sim 45°$ out of the plane of the sky.

In a previous paper (Kwok and Feldman 1981) we suggested that the radio source in GL 618 represents an ionization-bounded PN shell expanding into the remnant circumstellar envelope of its red-giant progenitor. This interpretation is supported by the detection of shock-excited H_2 emission (Beckwith, Persson, and Gatley 1978; Thronson 1981) as well as by the very high emission measure of the H II region. In this paper we report results on the radio structure of GL 618 from observations taken at the Very Large Array (VLA) of NRAO at three wavelengths (6, 2, and 1.3 cm) with resolutions ranging from a few arc seconds to $\sim 1/20$ of an arc second.

II. OBSERVATIONS AND RESULTS

GL 618 was observed in a "snap-shot" mode on six occasions at the VLA over a period of 16 months (1981 May–1982 September). Two out of the six observing sessions were made with hybrid configurations when the array was being changed from one standard configuration to another. With the exception of the 1981 August session, the array configurations were reasonably symmetric, and the synthesized beams approximately circular. The exact dates of observation and the array configurations are given in Table 1.

GL 618 was observed at all four standard VLA frequency bands (20, 6, 2, and 1.3 cm) during the 1981 observing sessions, but the 20 cm band was omitted in 1982 because of our failure to make a detection at this wavelength on the previous occasions. The on-source integration time spent at each frequency band was different in each observing session but was in all cases between 15 and 30 minutes. In addition, 3C 119 was observed before and after each source measurement at each frequency for calibration purposes. The absolute flux density was calibrated by observing 3C 48 at the beginning of each observing session.

The calibrated visibility data were recorded on magnetic tape at the VLA site, and further data processing was performed using standard VLA software, both at the University of Toronto and at the National Research Council, Ottawa. The source positions and angular sizes were determined by fitting elliptical Gaussian components to the calibrated visibility data. The results are given in Table 1. Also given in Table 1 are the smallest beam sizes achievable in the array configurations with which the observations were taken.

The calculated angular sizes and position angles in all

[1] The National Radio Astronomy Observatory (NRAO) is operated by Associated Universities, Inc., under contract with the National Science Foundation.

[2] The distance D is assumed to be 1.5 kpc.

TABLE 1

DERIVED POSITIONS, FLUX DENSITIES, AND ANGULAR SIZES OF GL 618

Observing Date	Configuration	Wavelength (cm)	Maximum Resolution (arc second)	Peak Flux at Maximum Resolution (mJy)	Summation of CLEANed Components (mJy)	Major Axis (arc second)	Minor Axis (arc second)	Position Angle	α(1950)	δ(1950)
1981 May 15	B	20	3.2	<4	...[a]	...	...	...	...	...
		6	1.05	...	...	0.63 ± 0.05	0.31 ± 0.09	73 ± 8	$04^h39^m34^s.021 \pm 0^s.001$	36°01′15″.93 ± 0″.01
		2	0.44	...	...	0.52 ± 0.08	0.29 ± 0.07	103 ± 14	34.017 ± 0.002	15.91 ± 0.02
		1.3	0.25	...	...	0.44 ± 0.06	0.26 ± 0.04	71 ± 10	34.021 ± 0.002	15.87 ± 0.01
1981 Aug 26	B → D	20	63 × 5	<7	...	...	...	...	...	...
		6	13 × 1.7	15.1 ± 0.3	15.7 ± 0.5	2.32 ± 1.68	0.0 ± 0.29	89 ± 6	$04^h39^m34^s.008 \pm 0^s.014$	36°01′15″.83 ± 0″.03
		2	4.2 × 0.6	85 ± 2	110 ± 4	0.0 ± 0.44	0.0 ± 0.08	76 ± 1	34.026 ± 0.002	15.91 ± 0.01
		1.3	2.8 × 0.4	145 ± 3	201 ± 10	0.84 ± 0.16	0.0 ± 0.06	87 ± 2	34.061 ± 0.002	15.89 ± 0.01
1981 Dec 23	C	20	10.1	<4	...	...	...	...	...	...
		6	3.5	17.1 ± 0.4	15.6 ± 0.5	0.80 ± 0.31	0.0 ± 1.05	149 ± 25	$04^h39^m34^s.031 \pm 0^s.002$	36°01′15″.85 ± 0″.03
		2	1.2	93.6 ± 1.0	106 ± 2	0.61 ± 0.03	0.19 ± 0.08	112 ± 5	34.028 ± 0.001	15.89 ± 0.01
		1.3	0.8	161.7 ± 1.5	203 ± 5	0.40 ± 0.02	0.13 ± 0.06	85 ± 4	34.030 ± 0.001	15.92 ± 0.01
1982 Jan 26	C → A	6	2.5	15.9 ± 0.2	16.9 ± 0.5	0.97 ± 0.18	0.23 ± 0.05	77 ± 4	$04^h39^m34^s.028 \pm 0^s.002$	36°01′15″.87 ± 0″.01
		2	1.5	89.6 ± 2.0	117 ± 3	0.58 ± 0.07	0.17 ± 0.02	58 ± 7	34.028 ± 0.001	15.87 ± 0.01
		1.3	1.1	191 ± 3	225 ± 3	0.49 ± 0.06	0.16 ± 0.10	86 ± 9	34.018 ± 0.001	15.87 ± 0.01
1982 Jun 24	A	6	0.35	12.38 ± 0.15	16.5 ± 0.5	0.73 ± 0.01	0.10 ± 0.01	86 ± 1	$04^h39^m34^s.037 \pm 0^s.001$	36°01′15″.87 ± 0″.01
		2	0.12	14.3 ± 0.6	73 ± 2	0.43 ± 0.01	0.12 ± 0.01	83 ± 1	34.033 ± 0.001	15.88 ± 0.01
		1.3	0.07	21.7 ± 1.0	214 ± 7	0.37 ± 0.01	0.11 ± 0.01	83 ± 1	34.030 ± 0.001	15.88 ± 0.01
1982 Sep 15	B	6	1.05	12.00 ± 0.24	13.9 ± 1	0.65 ± 0.04	0.26 ± 0.09	90 ± 6	$04^h39^m34^s.031 \pm 0^s.001$	36°01′15″.90 ± 0″.01
		2	0.39	57.9 ± 1.0	91 ± 2	0.44 ± 0.01	0.13 ± 0.02	87 ± 2	34.025 ± 0.001	15.92 ± 0.01
		1.3	0.22	82.7 ± 3.5	170 ± 6	0.33 ± 0.01	0.11 ± 0.02	83 ± 2	34.024 ± 0.001	15.91 ± 0.01
Weighted average						0.72 ± 0.01	0.11 ± 0.02	86 ± 2	$04^h39^m34^s.030 \pm 0^s.003$	36°01′15″.89 ± 0″.01
						0.45 ± 0.02	0.13 ± 0.01	81 ± 3	34.028 ± 0.002	15.89 ± 0.02
						0.36 ± 0.02	0.12 ± 0.02	84 ± 1	34.027 ± 0.004	15.88 ± 0.02

[a] Flux density information unavailable because of calibration procedure error.

frequency bands show that the source is clearly elongated along the E-W direction in line with the two visible nebulosities. There has been no detectable change in angular size over the period covered by the observations (16 months). Because of the changing array configurations, accurate comparison of the angular sizes obtained in different observing sessions is difficult. However, in the best case (1.3 cm) the major axis probably did not change by more than 0".1 between 1981 May and 1982 September.

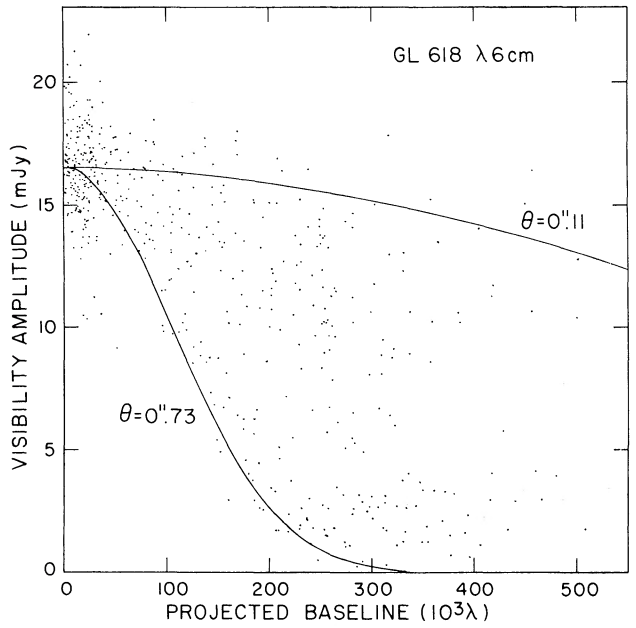

FIG. 1a

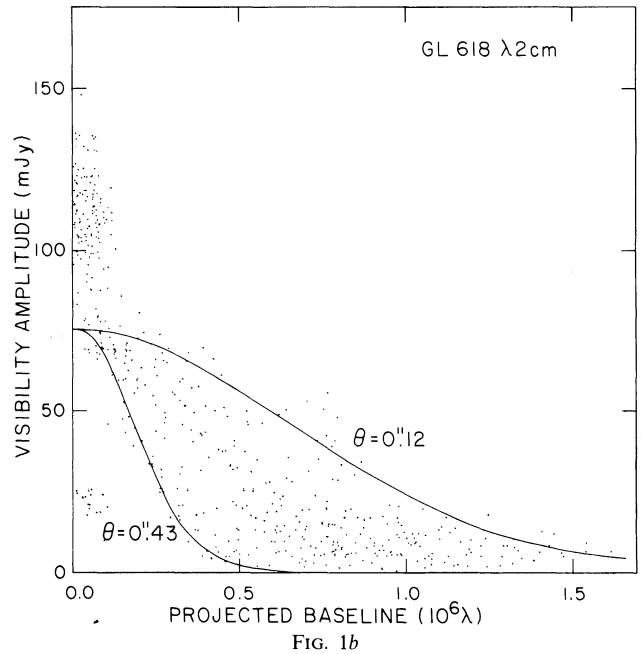

FIG. 1b

Although the minor axis of the radio emission is consistently found to be ~0".1 in length to half-intensity, the length of the major axis is found to increase with increasing wavelength. This suggests that GL 618 is ionization bounded in the N-S direction but not along the E-W direction. The wavelength dependence of the angular size implies different sizes of the optically thick surface at each frequency, suggesting a density gradient in the ionized region, or a core-halo structure.

The complex source structure of GL 618 can also be seen by plotting the visibility amplitudes against distance in the *u-v* plane. Figures 1*a*, 1*b*, and 1*c* show the visibility curves of GL 618 combining data taken at different sessions to improve the *u-v* coverage. While the 6 and 1.3 cm visibility plots could be approximated by elliptical Gaussians of different widths, the visibility plot of the 2 cm data (Fig. 1*b*) suggests a core-halo structure. The large apparent angular size of the source at 6 cm (0".7 × 0".1) compared with that at 1.3 cm (0".4 × 0".1) suggests that the emission is dominated by the halo at 6 cm, while the core is directly visible at 1.3 cm. We shall attempt to separate the contribution of these components and discuss each in turn.

a) The Core

Because of the expected high surface brightness of the core, it should be the dominant component at high frequencies, where the halo is optically thin. We have successfully resolved the core of GL 618 during the 1982 June session, when the VLA contained the greatest spacings and therefore had the highest angular resolution. Figures 2*a* and 2*b* show maps of GL 618 at 2 and 1.3 cm, respectively. The maps have been CLEANed to a level of 0.1 mJy at 2 cm and to 0.5 mJy at 1.3 cm. The respective beam sizes are 0".12 and 0".07. The 1.3 cm map indicates an elongated structure for the core.

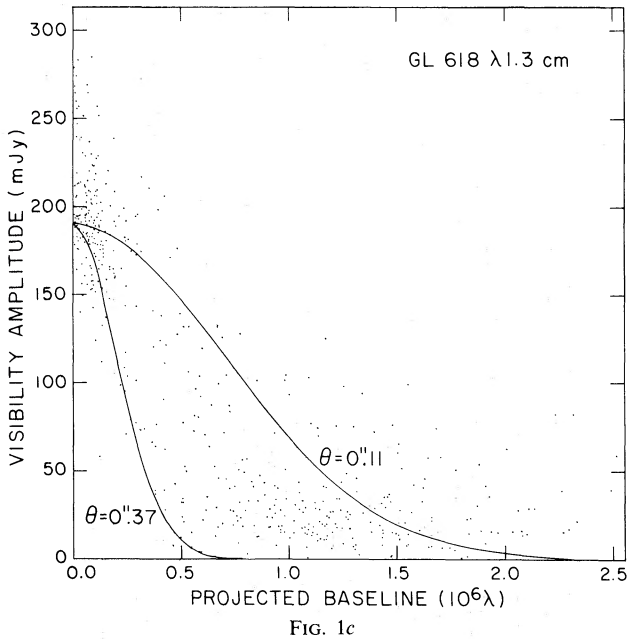

FIG. 1c

FIG. 1.—Combined visibility data of GL 618 in 1981 December, 1982 January, and 1982 June at (*a*) 6 cm, (*b*) 2 cm, and (*c*) 1.3 cm. The fringe amplitude is plotted against projected spacings within the array in units of wavelengths. Also plotted are two Gaussian curves representing the major and minor axes.

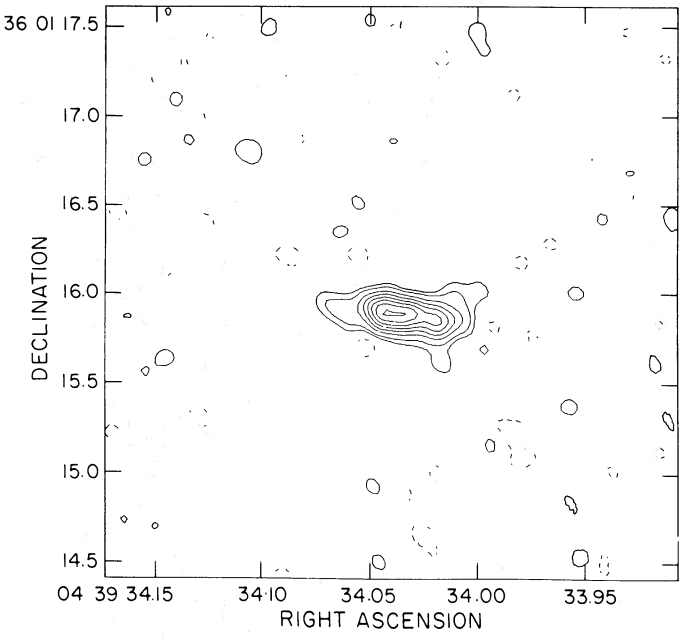

FIG. 2a

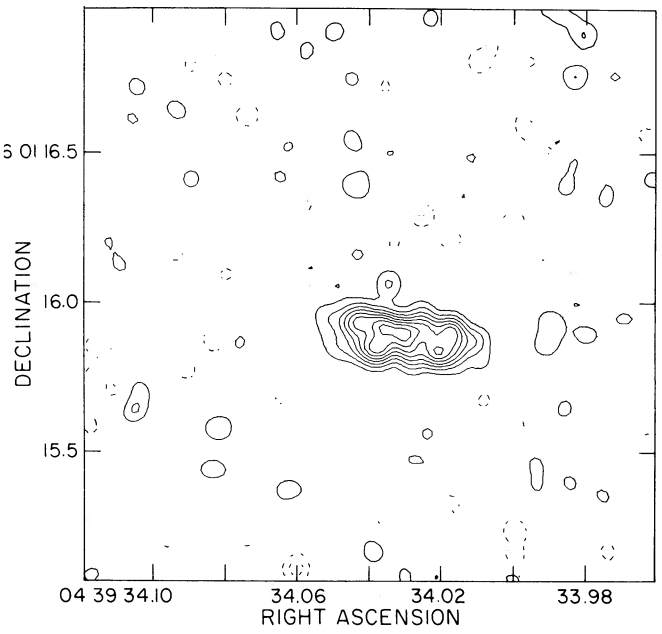

FIG. 2b

FIG. 2.—(*a*) CLEANed map of GL 618 (1982 June) at 2 cm. Contours are at intervals of 10% of the peak value (peak flux = 14.3 mJy per beam) with an additional contour at the 5% level. (*b*) CLEANed map of GL 618 (1982 June) at 1.3 cm. The contour intervals are 2.5 mJy per beam.

Its major axis is aligned exactly (within error) with the bipolar axis of the visible nebulosities. Although less structural information about the core can be obtained from the 2 cm map, the lowest contours of the map suggest the presence of extended emissions outside the compact core. The sensitivity limit of the map is ~0.5 mJy per beam, and we are unable to map the halo beyond several beamwidths from the core.

The integrated flux densities of the source in Figures 2*a* and 2*b* are 75 ± 3 and 188 ± 6 mJy, respectively. These values are obtained by summing all the CLEANed components which are removed from a rectangular box enclosing the source. We note that these values are smaller than the zero-spacing flux density amplitudes inferred from Figures 1*b* and 1*c*. In comparison, the total flux densities estimated from the 1981 December and 1982 January sessions are 108 ± 3 and 117 ± 5 mJy at 2 cm and 203 ± 4 and 212 ± 10 mJy at 1.3 cm. Since the synthesized beam sizes during the 1981 December and 1982 January sessions are more than 10 times the beam size during the 1982 June session, the difference in total flux density can be attributed to a contribution from a probable halo.

The flux density spectral index of the core component is $\alpha = 2.2 \pm 0.2$ ($S \propto \nu^{\alpha}$) between 2 and 1.3 cm, consistent with a blackbody spectrum. Since the core is optically thick to at least 22.5 GHz, a lower limit to the emission measure can be estimated (cf. Kwok, Purton, and Keenan 1981). Assuming an electron temperature of 2×10^4 K, the emission measure of the core must be $> 1.2 \times 10^{10}$ cm^{-6} pc. This implies a space density of 3×10^6 cm^{-3}, which is consistent with the absence of reflected forbidden lines (Schmidt and Cohen 1981). The estimated ionized mass is $\sim 3 \times 10^{-4}\ M_{\odot}$.

b) *The Halo*

Figures 3*a*, 3*b*, and 3*c* show 6 cm maps of GL 618 when observed with beam sizes of 0.″4, 0.″8, and 1.″4, respectively. This is accomplished by imposing a tapered function on the *u-v* plane. The source is semiresolved in all cases and is clearly not pointlike even in the lowest resolution case (Fig. 3*c*). The increase in peak flux density with beam size from 7.3 mJy in Figure 3*a* to 14.9 mJy in Figure 3*c* provides further evidence for an extended halo.

There is also marginal evidence for a monotonic increase in total 6 cm flux density from 14 mJy in 1980 March to 17 mJy in 1982 June. Although this change in flux is significant compared with the noise level in each observing session, we cannot rule out completely the possibility of systematic errors in calibration from one observing session to the next. In any case, this increase in flux density is considerably smaller than the rate of increase between 1977 and 1980 (Kwok and Feldman 1981), suggesting the expansion of the ionized region has slowed down.

The observed flux density at 6 cm (17 mJy) is higher than the expected flux density of the core (~8 mJy). This again suggests that the radio emission at 6 cm is dominated by an optically thick halo. From Figure 3*a* we can see that the halo is also elongated in the same direction as the core.

The total flux densities (core + halo) can be estimated from the peak flux densities in the lower resolution maps, by taking the summation of all the components removed during the CLEANing process, or from the zero-spacing flux amplitudes extrapolated from the visibility curves. Figure 4 shows the dependence of the peak fluxes on the beam size at all three observing frequencies. The total flux densities can be inferred

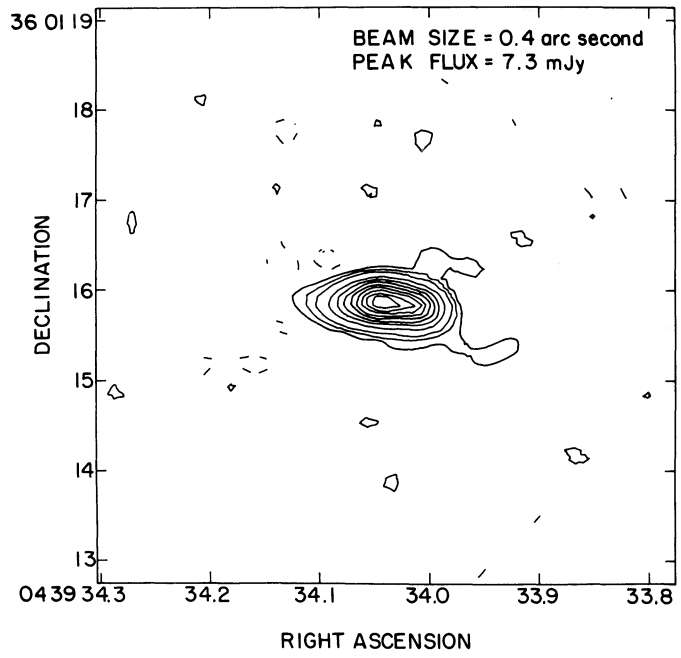

FIG. 3a

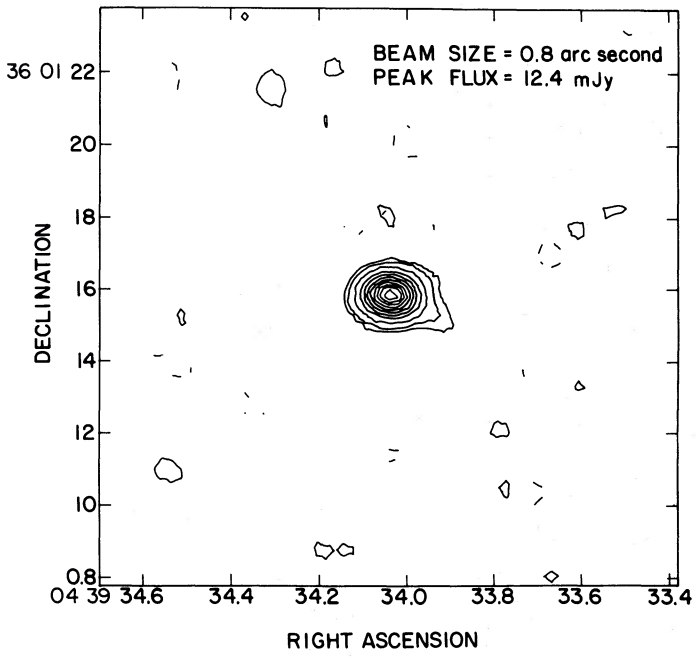

FIG. 3b

FIG. 3.—CLEANed 6 cm maps of GL 618 (1982 June) at different resolutions. Contours are at 10% of the peak value. (*a*) Beam size = 0.″4. Peak flux = 7.3 mJy per beam. Additional contours at 3% and 6% levels. (*b*) Beam size = 0.″8. Peak flux = 12.4 mJy per beam. Additional contours at 2% and 4% levels. (*c*) Beam size = 1.″4. Peak flux = 14.9 mJy per beam. Additional contours at 2% and 4% levels.

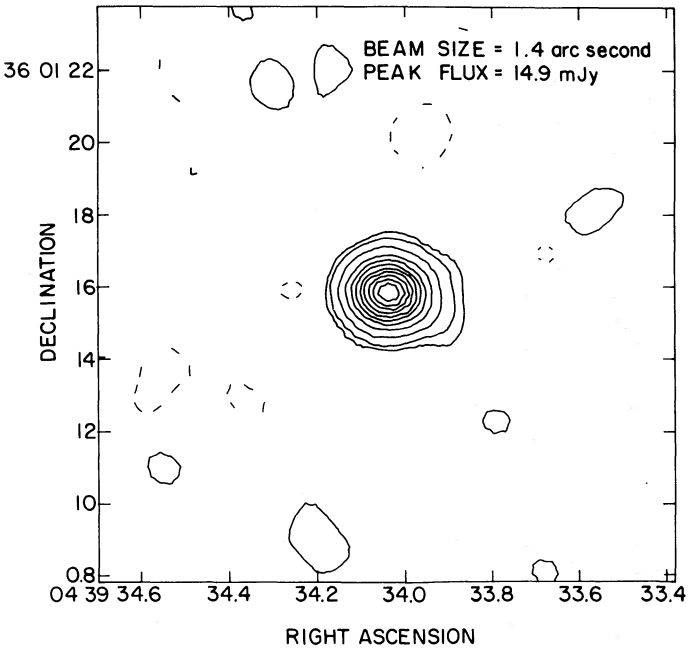

FIG. 3c

from the asymptotic values at large beam sizes and are found to be 17 ± 1, 100 ± 10, and 200 ± 15 mJy at 6, 2, and 1.3 cm, respectively. Total flux densities obtained from the summation of CLEANed components are less reliable, and this is evident in the variations seen in the sixth column of Table 1. Such systematic changes from one session to another can in part be attributed to the difference in the choice of CLEAN area due to the changing angular resolution. From the visibility curves in Figure 1, we estimate the zero-spacing flux density amplitudes to be 17 ± 2, 110 ± 10, and 210 ± 15 mJy for 6, 2, and 1.3 cm, respectively. Generally, all three methods give consistent results. Assigning subjective weightings to the results of each method, we come to the following estimates of the total flux densities:

$$S(6\text{ cm}) = 17 \pm 1\text{ mJy},$$

$$S(2\text{ cm}) = 110 \pm 10\text{ mJy},$$

$$S(1.3\text{ cm}) = 215 \pm 10\text{ mJy}.$$

Contributions from the halo component at 2 and 1.3 cm can be estimated by subtracting the core component from the total flux density assuming the halo is optically thin at these frequencies. We obtain 35 ± 5 mJy for the halo at both bands, which is consistent with the optically thin assumption. This value is, however, much larger than the total flux density at 6 cm, implying that the halo, as well as the core, is optically thick at wavelengths longer than 2 cm.

The spectra of the core and halo components are displayed in Figure 5. Also included in the figure is a single-dish measurement at 2.8 cm made at the Algonquin Radio Observatory.[3] Extrapolating the core spectrum to this wavelength, we find that an approximately equal contribution from the halo is required. It appears from Figure 5 that the spectral index of the halo is significantly less than 2 and is possibly consistent with the spectral index expected of a stellar wind situation (cf. Wright and Barlow 1975).

[3] The Algonquin Radio Observatory is operated by the National Research Council of Canada, Ottawa, as a national radio astronomy facility.

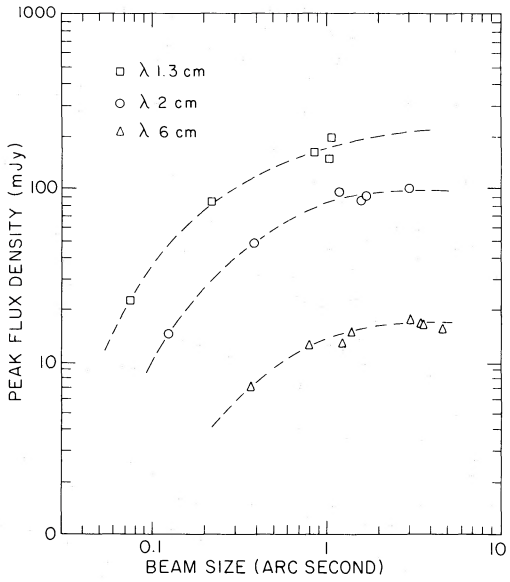

FIG. 4.—Peak flux densities estimated from CLEANed maps as a function of beam sizes. Typical 1 σ errors are 0.5, 1, and 5 mJy for 6, 2, and 1.3 cm, respectively. In addition, there may be systematic errors due to calibrations, atmospheric conditions, etc. Also drawn are eye-fitted curves to data of each wavelength showing the general dependence on beam sizes.

III. DISCUSSION

We have found that the radio core of GL 618 has an elongated structure along the same axis as the visible nebulosities. This suggests that the radio and visible components belong to the same bipolar structure which extends from 0.″2 to 4″ on each side of the central star (Fig. 6). Two questions naturally arise from this picture: (1) Is the bipolar nature of GL 618 a result of preferential ejections along certain directions? (2) What causes the higher emission measure in the radio core? We shall now proceed to answer these questions within the framework of the interacting-winds model of PN formation.

PNs with bipolar morphology have long been known, and it seems reasonable to attempt to establish a connection between the bipolar character of GL 618 and bipolar PNs. Peimbert and Torres-Peimbert (1983) find that bipolar PNs often have high [He]/[H] and [N]/[O] abundance ratios, which implies in turn that their progenitors must have had main-sequence masses in excess of 2 $M_\odot$. The fact that GL 618 is nitrogen rich (Calvet and Peimbert 1983) is consistent with this hypothesis. Furthermore, even if the high rate of AGB mass loss ($\dot{M} \approx 2 \times 10^{-4}\ M_\odot\ \mathrm{yr}^{-1}$, Knapp *et al.* 1982) in this object has lasted for only 10^4 yr, there should be $\sim 2\ M_\odot$ of wind material in the remnant RGE. This again suggests that GL 618 has a high-mass progenitor.

The above morphology-mass connection is further explored by Calvet and Peimbert (1983), who note that high-mass main-sequence stars have high rotation velocities, and a large part of their angular momentum can be lost on the AGB with the onset of mass loss. The stellar wind will concentrate on the equatorial plane, and an anisotropic circumstellar envelope will be created. When the central star evolves to the PN stage, a new fast wind is generated which will interact with the remnant RGE and create a bipolar nebula along the axis of rotation.

It is now widely recognized that the interaction of stellar winds plays an important role in the formation and evolution of PNs (Kwok 1982), and bipolar nebulae provide an interesting special case to illustrate this process. For example, the bipolar appearance of NGC 6302 can be explained by the interacting-winds process (Meaburn and Walsh 1980), and the detection of neutral hydrogen outside the visible nebula by

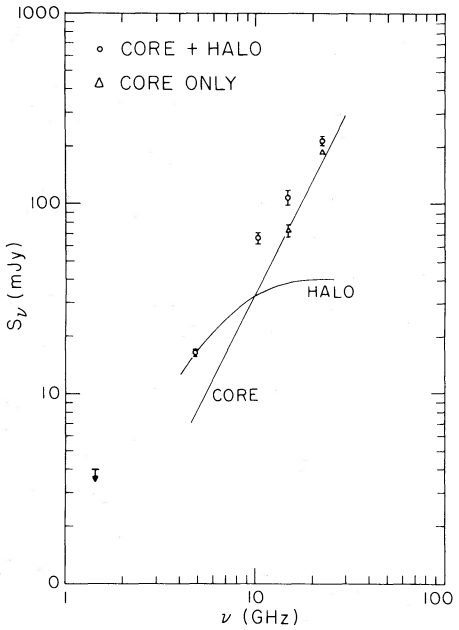

FIG. 5.—Spectra of GL 618 in early 1982

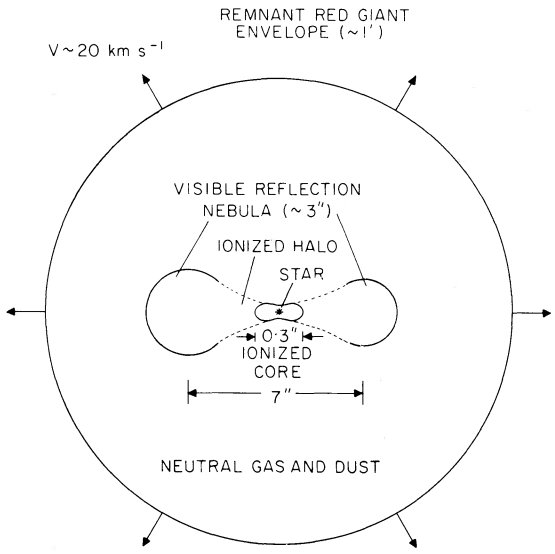

FIG. 6.—A schematic diagram of GL 618 (not to scale)

Rodríguez and Moran (1982) gives strong support to this picture.

Although the bipolar morphology of GL 618 is on a much smaller scale than NGC 6302, a model similar to that of Meaburn and Walsh (1980) may also apply to GL 618. Since the density in the radio core of GL 618 is much higher than the densities of the visible lobes, the visible reflection nebulae may be identified as part of the remnant circumstellar envelope ejected while the star was on the AGB, but they are now ionized by the central star. This can be the result of a rapid expansion of the ionization front along the bipolar axis, while the envelope remains neutral in other directions. Again, an anisotropic density distribution in the remnant RGE could be responsible for the preferential expansion of the ionization front. The core then represents the nascent PN shell, or the contact discontinuity in the interacting-stellar winds model of Kwok, Purton, and FitzGerald (1978).

Since the mass of the molecular envelope ($\gtrsim 2\ M_\odot$) of GL 618 is much larger than the mass of the H II region ($< 10^{-3}\ M_\odot$), the red-giant wind must have terminated not too long ago. If the radio core indeed represents the interface of molecular and ionized gas, then the expansion velocity of 18 km s^{-1} (Knapp *et al.* 1982) implies a termination of the AGB mass loss no more than 100 yr ago. This is consistent with the optical history of GL 618, which was below the detection limit of the Sky Survey prints of Harvard Observatory until 1940 and has since undergone a steady increase in brightness of 0.06 mag yr^{-1} (Gottlieb and Liller 1976). This again argues against a low-mass central star, since a 0.6 $M_\odot$ central star would take between 3000 and 10,000 yr to reach a temperature of 3×10^4 K from the AGB (Renzini 1983). If we adopt a distance of 1.5 kpc, then the luminosity of GL 618 implies a central stellar mass of 0.8 $M_\odot$ (Paczyński 1971). In this case, the central star temperature of GL 618 could increase tenfold to 3×10^5 K in the next 100 yr (Paczyński 1971), completely changing its present ionization structure. This time scale would be even shorter if the mass loss rate from the central star is comparable to its nuclear-burning rate of $\sim 3 \times 10^{-7}\ M_\odot\ yr^{-1}$.

IV. CONCLUSIONS

GL 618 was observed at the VLA under different array configurations and therefore with different angular resolutions. The results suggest a core-halo structure for the ionized region of GL 618. With beam sizes as small as 0".07, we were able to resolve the core and found it to have an E-W elongated structure (size 0".4 × 0".1). The visible bipolar nebulosities appear to be extensions of the radio core and could be the result of a preferential expansion of the ionization front along the bipolar axis.

We suggest that GL 618 is a proto-PN whose rotating red-giant progenitor had been ejecting wind material predominantly in the equatorial plane. The high densities in the equatorial directions prevent the UV photons emitted by the 30,000 K central star from penetrating into the remnant RGE, and the resultant unbalanced resistance to the ionization front creates the bipolar morphology.

Consistent with the model of Calvet and Peimbert (1983) for bipolar PNs, GL 618 is likely to have descended from a high-mass progenitor (main-sequence mass $\gtrsim 3\ M_\odot$). The present mass ($\sim 0.8\ M_\odot$) of its central star is high compared with most PNs (Schönberner and Weidemann 1983), and the star is expected to undergo rapid evolution in the next several hundred years.

We would like to thank Ms. Peggy Perley, who skillfully calibrated most of the data presented here. S. K. also wishes to thank Dr. Philipp Kronberg for use of the VLA data reduction facility at the University of Toronto. Discussions with Drs. J. M. MacLeod and H. E. Matthews are gratefully acknowledged.

REFERENCES

Beckwith, S., Persson, S. E., and Gatley, I. 1978, *Ap. J.* (*Letters*), **219**, L33.
Calvet, N., and Cohen, M. 1978, *M.N.R.A.S.*, **182**, 687.
Calvet, N., and Peimbert, M. 1983, *Rev. Mexicana Astr. Ap.*, Vol. 5, No. 4, 319.
Carsenty, V., and Solf, J. 1982, *Astr. Ap.*, **106**, 307.
Gottlieb, E. W., and Liller, W. 1976, *Ap. J.* (*Letters*), **207**, L135.
Kleinmann, S. G., Sargent, D. G., Moseley, H., Harper, D. A., Loewenstein, R. F., Telesco, C. M., and Thronson, H. A. 1978, *Astr. Ap.*, **65**, 139.
Knapp, G. R., Phillips, T. G., Leighton, R. B., Lo, K. Y., Wannier, P. G., Wootten, H. A., and Huggins, P. J. 1982, *Ap. J.*, **252**, 616.
Kwok, S. 1982, *Ap. J.*, **258**, 280.
Kwok, S., and Feldman, P. A. 1981, *Ap. J.* (*Letters*), **267**, L67.
Kwok, S., Purton, C. R., and FitzGerald, M. P. 1978, *Ap. J.* (*Letters*), **219**, L125.
Kwok, S., Purton, C. R., and Keenan, D. W. 1981, *Ap. J.*, **250**, 232.
Lo, K. Y., and Bechis, K. P. 1976, *Ap. J.* (*Letters*), **205**, L21.
Meaburn, J., and Walsh, J. R. 1980, *M.N.R.A.S.*, **191**, 5P.
Paczyński, B. 1971, *Acta Astr.*, **31**, 417.
Peimbert, M., and Torres-Peimbert, S. 1983, in *IAU Symposium 103, Planetary Nebulae*, ed. D. R. Flower (Dordrecht: Reidel), p. 233.
Renzini, A. 1983, in *IAU Symposium 103, Planetary Nebulae*, ed. D. R. Flower (Dordrecht: Reidel), p. 267.
Rodríguez, L. F., and Moran, J. M. 1983, *Nature*, **229**, 323.
Schmidt, G. D., and Cohen, M. 1981, *Ap. J.*, **246**, 444.
Schönberner, D., and Weidemann, V. 1983, in *IAU Symposium 103, Planetary Nebulae*, ed. D. R. Flower (Dordrecht: Reidel), p. 359.
Thronson, H. A. 1981, *Ap. J.*, **248**, 984.
Westbrook, W. E., Becklin, E. E., Merrill, K. M., Neugebauer, G., Schmidt, M., Willner, S. P., and Wynn-Williams, C. G. 1975, *Ap. J.*, **202**, 407.
Wright, A. E., and Barlow, M. J. 1975, *M.N.R.A.S.*, **170**, 41.
Wynn-Williams, C. G. 1977, *M.N.R.A.S.*, **181**, 61P.

Note added in proof.—We have found a possible calibration error in the 2 cm data of the 1982 June session which may have caused the 2 cm flux density to have been underestimated by as much as 30%. If this is the case, then the flux contribution of the halo may be less than that suggested in the paper.

R. C. BIGNELL: National Radio Astronomy Observatory, P.O. Box 0, Socorro, NM 87801

S. KWOK: Department of Physics, University of Calgary, Calgary, Alberta T2N 1N4, Canada